Delft University of Technology

Measuring plastic deformation in epitaxial silicon after thermal oxidation

Sweers, K. V.; Kuppens, P. R.; Tolou, N.

DOI
10.1109/MARSS.2019.8860984

Publication date
2019

Document Version
Final published version

Published in
Proceedings of MARSS 2019

Citation (APA)
Sweers, K. V., Kuppens, P. R., & Tolou, N. (2019). Measuring plastic deformation in epitaxial silicon after thermal oxidation. In S. Haliyo, A. Sill, Q. Zhou, P. Kallio, & S. Fatikow (Eds.), *Proceedings of MARSS 2019: 4th International Conference on Manipulation, Automation, and Robotics at Small Scales* IEEE. https://doi.org/10.1109/MARSS.2019.8860984

Important note
To cite this publication, please use the final published version (if applicable).
Please check the document version above.

Copyright
Other than for strictly personal use, it is not permitted to download, forward or distribute the text or part of it, without the consent of the author(s) and/or copyright holder(s), unless the work is under an open content license such as Creative Commons.

Takedown policy
Please contact us and provide details if you believe this document breaches copyrights.
We will remove access to the work immediately and investigate your claim.

This work is downloaded from Delft University of Technology.
For technical reasons the number of authors shown on this cover page is limited to a maximum of 10.

Green Open Access added to TU Delft Institutional Repository

'You share, we take care!' - Taverne project

https://www.openaccess.nl/en/you-share-we-take-care

Otherwise as indicated in the copyright section: the publisher is the copyright holder of this work and the author uses the Dutch legislation to make this work public.

Measuring plastic deformation in epitaxial silicon after thermal oxidation*

K. V. Sweers[1], P. R. Kuppens[2], and N. Tolou[3]

Abstract— **Residual stress from thermal oxidation can cause plastic deformation in silicon microelectromechanical systems (MEMS). This paper presents a novel method to distinguish elastic and plastic strain in silicon beams, by removing the oxide layer to show the plastic strain. A lever mechanism is used as a mechanical amplifier. The plasticity model by Alexander and Haassen (AH) is used in a numerical model to predict the elastic and plastic strain. Experiments in epitaxially grown silicon show significantly less plastic strain than predicted by the model. We conclude that the AH model is not valid for epitaxially grown silicon with very little initial dislocations. Since epitaxially grown silicon generally has less dislocations compared to floating zone silicon we recommend using the former when plastic deformation is to be avoided.**

I. Introduction

Thermal oxidation in silicon microelectromechanical systems (MEMS) induces stress in the oxide film and bulk silicon. This residual stress causes deformations in the silicon, which can be partially plastic under certain conditions. These plastic deformations are not completely understood yet. Some effects of residual stress in MEMS include damage [1], warpage [2], reduced sensitivity of ultrasonic sensors [3], and buckling [4].

Thermal oxide is typically used as a sacrificial layer in the etch process, or for electrical insulation. It is grown in an oxygen rich environment, at high temperatures typically ranging from 800 °C to 1200 °C. At these high temperatures silicon behaves ductile, in contrast to the very brittle behavior at room temperature [5]. Usually the film is very thin compared to the silicon bulk, so stress in the bulk is low and no plastic strain occurs. For relative thicker oxide compared to the bulk, significant plastic deformation can be expected.

Literature provides many methods to measure residual stress and strain in thin films. The most common method is to measure the wafer curvature [6], [7], and calculate thin film stress using the Stoney equation [8]. Some of other commonly used methods include buckling beams [9]–[11], piezo [12], [13], motion amplifying mechanisms [14]–[17], and x-ray diffraction [18], [19]. Although these studies all measure strain, none make the distinction between elastic and plastic strain.

Measurements of the plastic behavior of oxidized thin silicon beams have not been done before. Better understanding of this behavior gives designers the insight to either avoid or exploit plastic deformation after oxidation. It could be used to permanently deform silicon members in a passive way, contrary to [20] and [21] who used active mechanical contact to obtain plastic deformations. Another application is to create preloading in silicon members [22]. This can be used to remove clearance between components or to apply preloading. Potential applications are energy harvesters and MEMS accelerometers [23].

This paper presents elastic and plastic strain measurements in epitaxial silicon beams, as a result of thermal oxidation. A novel measurement method is used to distinguish elastic and plastic strain, by removing the oxide film to show the plastic strain. A lever mechanism is used as a mechanical amplifier. Experiments are performed with different beam widths and oxidation temperatures. A numerical model is implemented to predict elastic and plastic strain, which are compared to experimental results.

The working principle and design of the lever mechanism, as well as the modeling, are described in section II. Experimental and theoretical results are presented in section III. The results are discussed in section IV and a conclusion is given in section V.

II. Methods

A. Working principle

A silicon dioxide film is grown on the surfaces of silicon beams at elevated temperatures. It was shown by [24] that silicon dioxide grows in a stress free state above the viscous flow point, which is between 950 °C and 975 °C. It is therefore assumed that the only cause for stress is the difference of coefficient of thermal expansion (CTE) between silicon dioxide and silicon. A surface stress will be induced when the specimen cools down to room temperature. This surface stress in the silicon dioxide film induces a net axial tensile stress in the silicon cantilever beam. This stress causes elongation of the beam, which can have a plastic component besides an elastic one. Plastic deformation can theoretically occur if there is sufficient stress above the brittle-ductile transition temperature [25]. In thicker beams less stress is induced, and they will stretch less than thinner beams. The total strain, which can be measured at room temperature, is the sum of elastic and plastic strain. To distinguish these,

*This research is conducted at the instigation of and with close collaboration of TAG Heuer Institute, La Chaux de Fonds, 2300 Switzerland, and its Director, Mr G.A.(Guy) Sémon, and received funding from TAG Heuer Institute.

[1]K. V. Sweers is with Faculty of Mechanical, Maritime and Materials Engineering, Delft University of Technology, Delft, Mekelweg 2, The Netherlands kornesweers@gmail.com

[2]P. R. Kuppens is with Faculty of Mechanical, Maritime and Materials Engineering, Delft University of Technology, Delft, Mekelweg 2, The Netherlands P.R.Kuppens@tudelft.nl

[2]N. Tolou is with Faculty of Mechanical, Maritime and Materials Engineering, Delft University of Technology, Delft, Mekelweg 2, The Netherlands N.Tolou@tudelft.nl

978-1-7281-0948-0/19/$31.00 ©2019 IEEE

Authorized licensed use limited to: TU Delft Library. Downloaded on February 18,2021 at 07:29:10 UTC from IEEE Xplore. Restrictions apply.

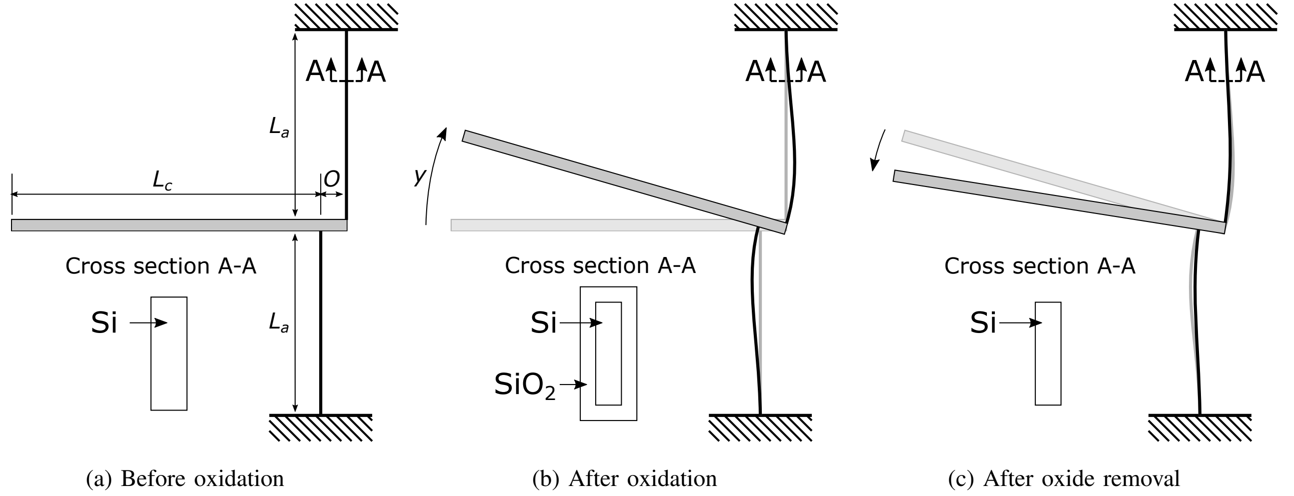

(a) Before oxidation (b) After oxidation (c) After oxide removal

Fig. 1: Working principle of the lever mechanism. Fig. 1a shows the initial position, before oxidation. Fig. 1b shows the position after oxidation. The beam rotates with tip displacement y because of the stress in beams L_A. After the oxide is removed, the elastic component of the strain is released. Only plastic deformation remains, which is shown in Fig 1c.

the oxide film is removed in our method. This eliminates the source of stress in the silicon beam, so only the plastic strain remains.

Elastic and plastic strains are expected to be in the order of $0.01\,\%$. Without amplification, this would result in elongations in the order of $0.1\,\mu\text{m}$ for $1\,\text{mm}$ long beams, which is hard to measure. Therefore a lever mechanism is used to amplify the displacement, and obtain a sufficient measurement resolution. This type of mechanism is well known for stress measurements in thin films [14]–[17]. In these devices, the mechanism is etched in the thin film only. When it is freed from the underlying sacrificial layer, the film stress is released, causing the mechanism to rotate.

In this work, the mechanism is etched in a layer of epitaxial silicon, after which a silicon dioxide film is grown on all surfaces of the mechanism. The working principle of this mechanism is schematically shown in Fig. 1. Strain in beams L_a cause beam L_c to rotate. The small gap O and length of L_c amplifies this rotation. The rotation is observed at the tip of the rotating beam, and is used to calculate the strain in beams L_a.

A vernier scale at the tip of the rotating beam is used to allow for easy read out of tip displacement under an optical microscope. An example measurement can be seen in Fig. 5c.

The kinematic relation between strain ε and tip displacement y is given by [17] :

$$\varepsilon = \frac{y}{L_a \left(1 + 2\frac{L_c}{O}\right)} \tag{1}$$

For this relation, ideal joints are assumed. The dimensions are chosen based on fabrication and measurement limitations, and are $L_a = 1000\,\mu\text{m}$, $L_c = 4000\,\mu\text{m}$, and $O = 100\,\mu\text{m}$. The vernier scale is dimensioned to be observed with an optical microscope for the expected deformations with a resolution of $1\,\mu\text{m}$ tip displacement. With these dimensions, a strain resolution of $1.2 \times 10^{-3}\,\%$ is obtained.

A finite element method (FEM) analysis in COMSOL shows a deviation from this linear relation of Eq. 1 up to $0.0093\,\%$ strain in our measurement range. It is found that a correction factor in the form of the second order polynomial from eq. 2 gives a good fit to the FEM data. A least squares fit on the FEM data in the range of $0\,\%$ to $0.14\,\%$ strain gives values for C_1 and C_2 of 1.0235 and 442.9039. With this fit, the maximum error in this range is reduced to $0.0005\,\%$ strain. Eq. 2 is used to calculate the strain from experimental tip displacement data.

$$\varepsilon = \frac{C_1 y + C_2 y^2}{L_a \left(1 + 2\frac{L_c}{O}\right)} \tag{2}$$

To prevent the compressive load to buckle the mechanism sideways a linear and nonlinear buckling analysis is performed using the FEM model. Extreme values of beam widths and thermal loads (mention values) confirm the mechanism will rotate as desired.

B. Fabrication and measurements

A silicon on insulator (SOI) wafer is used with a $300\,\mu\text{m}$ thick handling layer, $2\,\mu\text{m}$ silicon dioxide layer, and a $50\,\mu\text{m}$ thick epitaxial silicon device layer in the (100) orientation. Deep reactive ion etching (DRIE) is used to etch the lever mechanisms in the epitaxial silicon layer from the front. It is assumed that DRIE does not induce stress in the mechanism. DRIE is also used to etch a cavity in the handling layer to release the mechanisms. Samples are made with beams aligned to the <100> and <110> directions.

A $10\,\text{mm}$ x $10\,\text{mm}$ stepper mask is used. Each sample contains six rotating beams, as can be seen in Fig. 2 and Fig. 4. Devices are fabricated with beam widths of $6.48\,\mu\text{m}$, $11.48\,\mu\text{m}$, and $16.48\,\mu\text{m}$, where overetching and consumed silicon by the silicon dioxide are considered. The target widths of the silicon beams after oxidation are $5\,\mu\text{m}$, $10\,\mu\text{m}$, and $15\,\mu\text{m}$ (without silicon dioxide). Each sample contains

Authorized licensed use limited to: TU Delft Library. Downloaded on February 18,2021 at 07:29:10 UTC from IEEE Xplore. Restrictions apply.

two devices of each beam width. Markers are etched to identify the beam width and to read the displacement on the scale, see Fig. 5.

A silicon dioxide layer of $1\,\mu m$ thick is grown using wet thermal oxidation at $900\,°C$, $950\,°C$, $1000\,°C$, $1050\,°C$, and $1100\,°C$. The oxide film is grown on all silicon surfaces. The oxidation times are calculated using the Deal-Grove model [26]. The samples are placed horizontally in the furnace, eliminating in-plane gravity effects. After oxidation, the furnace cools to $800\,°C$. The samples are annealed at this temperature for about 16 hours before they are removed from the furnace. The temperature profile is shown in Fig. 3. The oxide thickness is measured with spectral reflectance using the Leitz MPV SP at 3 different locations across the front side of the sample. The oxide is removed with vapor hydrofluoric acid (VHF). As plastic deformation is expected during cooling, it is assumed that surface defects as a result of the VHF do not influence plastic deformation.

In each sample, the width of one $5\,\mu m$, $10\,\mu m$, and $15\,\mu m$ beam are measured with a Keyence VHX-6000 optical microscope at 3 locations along the beams. For one sample of <100> and <110>, the beam widths are also measured from the backside.

The strain measurement consists of multiple readouts in different stages of the fabrication process. The tip displacement is obtained by observing the vernier scales under a Keyence VHX-6000 optical microscope. An initial measurement is done before oxidation. The total strain, which is the sum of elastic and plastic strain, is measured after oxidation. The plastic strain is measured after the silicon dioxide is removed using the VHF.

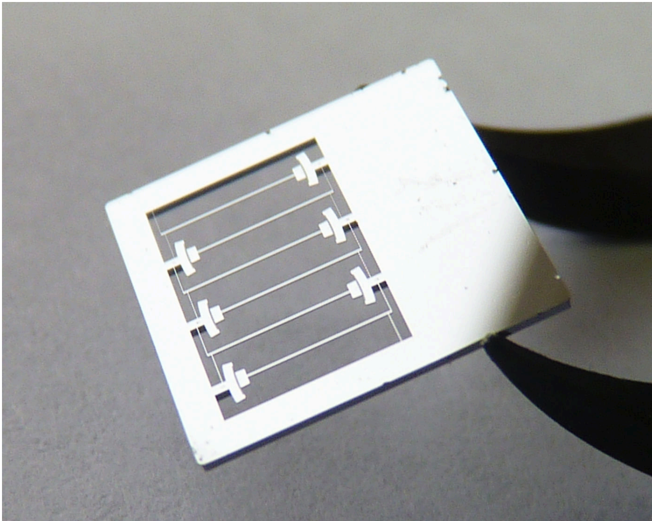

Fig. 2: Picture of a sample.

C. Modeling

Stress and strain during cooling in oxidized fixed-free silicon cantilever beams, oriented in the <100> and <110> directions, are numerically modeled in MATLAB. Elongation of the thin beams causes additional stress, originating from the bending of the thin beams. The FEM model of the lever mechanism shows that this stress is negligible compared to the thermal stress in the silicon, and thus validates the assumption of a fixed-free beam.

The total strain rate in silicon and silicon dioxide must be equal at their interface, and is assumed to be uniform throughout the cross section. The total strain rate for both materials consists of elastic, plastic and thermal strain rates. The total strain rate equation is given by:

$$\dot{\varepsilon}_{Si,th} + \dot{\varepsilon}_{Si,el} + \dot{\varepsilon}_{Si,pl} = \dot{\varepsilon}_{SiO_2,th} + \dot{\varepsilon}_{SiO_2,el} + \dot{\varepsilon}_{SiO_2,pl} \quad (3)$$

Where $\dot{\varepsilon}_{Si,th}$, $\dot{\varepsilon}_{Si,el}$ $\dot{\varepsilon}_{Si,pl}$ are the thermal, elastic, and plastic strain rates of the silicon, and $\dot{\varepsilon}_{SiO_2,th}$, $\dot{\varepsilon}_{SiO_2,el}$, and $\dot{\varepsilon}_{SiO_2,pl}$ the thermal, elastic and plastic strain rates of the silicon dioxide.

Plastic strain in silicon is governed by the movement of dislocations. As these crystallograhpic defects move, the lattice is rearranged causing permanent deformation. The silicon crystal structure contains 12 slip systems on which dislocations can move [27]. The resolved shear stress τ_r on a slip system is related to a tensile stress σ by the Schmid factor M:

$$\tau_r = \sigma M \quad (4)$$

M depends on the relative orientation of the tensile stress to the slip system. The slip systems with the highest resolved shear stress, and thus the highest Schmid factor, are considered active. The plastic strain rate for silicon is given by the Orowan equation [28]:

$$\dot{\varepsilon}_{Si,pl} = MnN_m vb \quad (5)$$

Where n is the number of active independent slip systems with Schmid factor M, N_m the mobile dislocation density for each slip system, v the average dislocation velocity, and b the length of the Burgers vector. The model by Alexander and Haassen (AH) is universally used to describe dislocation velocity and evolution of the dislocation density. The parameter values from [29] are used in this model. The dislocation velocity v is:

$$v = B_0 \left(\frac{\tau_{eff}}{\tau_0}\right)^m \exp\left(\frac{-Q}{k_b T}\right) \quad (6)$$

Where B_0 is a reference velocity equal to $4.3 \times 10^4\,\mathrm{m\,s^{-1}}$, τ_{eff} the effective shear stress, τ_0 a reference stress, Q the activation energy, k_b the Boltzmann constant, and T the temperature.

The effective shear stress τ_{eff} is given by:

$$\tau_{eff} = \left\langle \sigma M - \frac{Gb\sqrt{N_m}}{\beta} \right\rangle \quad (7)$$

Where G is the shear modulus, and β a parameter characterizing the interaction between dislocations. If $x > 0$, $\langle x \rangle = x$, and if $x \leq 0$, $\langle x \rangle = 0$. The dislocation density is

Authorized licensed use limited to: TU Delft Library. Downloaded on February 18,2021 at 07:29:10 UTC from IEEE Xplore. Restrictions apply.

assumed to increase proportionally to the area swept by the dislocations and the effective shear stress:

$$\dot{N}_m = K N_m v \tau_{eff} \tag{8}$$

Where K is a constant with value $3.1 \times 10^{-4}\,\mathrm{m\,N^{-1}}$.

Force equilibrium allows the axial stress in the silicon dioxide to be expressed by the stress in the silicon:

$$\sigma_{SiO_2} = \frac{-\sigma}{A_r} \tag{9}$$

Where σ_{SiO_2} is the axial stress in the silicon dioxide, and A_r the ratio of cross sectional area of silicon dioxide over silicon.

The plastic strain rate of silicon dioxide is modeled with a viscous flow model, as proposed by [30]. The plastic strain rate of the silicon dioxide is given by:

$$\dot{\varepsilon}_{SiO_2,pl} = \frac{-\sigma}{\eta A_r} \tag{10}$$

Where η is the temperature dependent viscosity [30].

Silicon is an anisotropic material, so the elastic modulus depends on the relative orientation to the crystal lattice. For uniaxial tension, the appropriate elasticity modulus E can be simplified to a single value [31]. The cantilever beams aligned with the <100> and <110> directions have elasticity moduli:

$$E_{si,100} = \frac{1}{s_{11}} \tag{11}$$

and

$$E_{si,110} = \frac{4}{2s_{11} + 2s_{12} + s_{44}} \tag{12}$$

where s_{11}, s_{12}, and s_{44} are components in the compliance tensor.

The second order temperature dependence of the components in the compliance tensor found by [32] are used in this study. Even though this relation is based on measurements at lower temperatures, similar values for higher temperatures are found in [33]. The elastic strain rate is given by:

$$\dot{\varepsilon}_{Si,el} = \frac{\dot{\sigma}}{E_{si}} \tag{13}$$

Silicon dioxide is modeled as an isotropic material. The elastic modulus E_{SiO_2} is assumed to independent of temperature with a value of $64\,\mathrm{GPa}$ [34]. The elastic strain rate for silicon dioxide is:

$$\dot{\varepsilon}_{SiO2,el} = \frac{-\dot{\sigma}}{A_r E_{SiO_2}} \tag{14}$$

The thermal strain rates for silicon and silicon dioxide depend on the cooling rate $\dot{T}$ and the thermal expansion coefficient. For silicon, the thermal strain rate is:

$$\dot{\varepsilon}_{Si,th} = \alpha_{Si} \dot{T} \tag{15}$$

Where α_{Si} is the thermal expansion coefficient for silicon. The empirical formula proposed by [35] for the temperature dependence of α_{Si} is used. Because the lateral strain is constrained by the silicon, there is an additional term in the axial thermal strain rate equation for silicon dioxide. The thermal strain rate is:

$$\dot{\varepsilon}_{SiO_2,th} = \alpha_{SiO_2} \dot{T} + (\alpha_{SiO_2} - \alpha_{Si})\, \nu \dot{T} \tag{16}$$

Where α_{Si} is the thermal expansion coefficient for silicon dioxide, and ν the Poisson ratio of silicon dioxide. The temperature dependence reported in [34] is used.

The cooling process is modeled by solving the differential equations 5, 8, 10, 13, 14, 15, and 16 numerically for $T(t)$ in MATLAB. The initial value for the dislocation density is assumed to be $1 \times 10^4\,\mathrm{cm^{-2}}$ [36], [37].

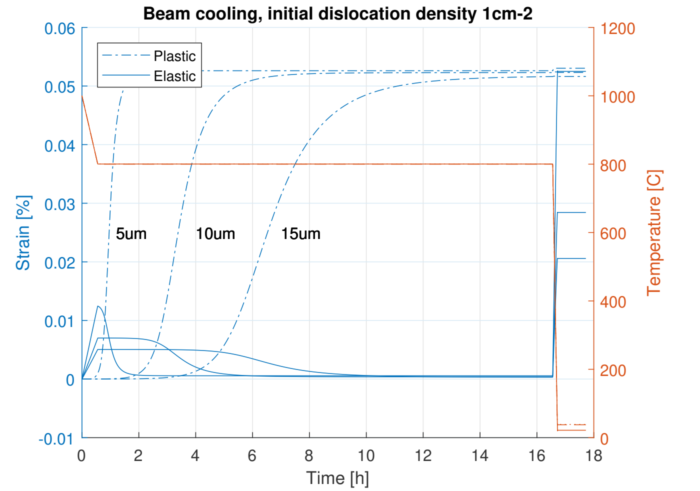

Fig. 3: Temperature profile for oxidation at $1000\,°\mathrm{C}$, and elastic and plastic strain during cooling. Plastic strain from left to right resemble the beams with $5\,\mu\mathrm{m}$, $10\,\mu\mathrm{m}$, and $15\,\mu\mathrm{m}$ respectively.

III. Results

A. Characterization

Fig. 2 and Fig. 4 show an example of a fabricated sample. The oxide thickness measurements can be seen in Tab. I. For the samples oxidized at $1100\,°\mathrm{C}$ the oxide thickness was very close to the target. For the other samples, there was an increasing deviation from the target for samples oxidized at lower temperatures. The average measured beam width from the front are shown in Tab. I. The beam widths of the samples oxidized at $1000\,°\mathrm{C}$ were also measured from the backside. The beam widths from the backside are on average $1.22 \pm 0.30\,\mu\mathrm{m}$ smaller compared to the front side. To calculate A_r, the measurements from the front side are corrected with this average.

B. Measurements

An example of a read out of the vernier scale is shown in Fig. 5. The elastic and plastic strain measurements for the <100> and <110> aligned samples are plotted in Fig. 6-10, together with simulation results with and without the plasticity model for silicon. In general, very little plastic strain was observed. An attempt to obtain larger plastic strains was made by growing $2\,\mu\mathrm{m}$ oxide films at $1100\,°\mathrm{C}$,

Authorized licensed use limited to: TU Delft Library. Downloaded on February 18,2021 at 07:29:10 UTC from IEEE Xplore. Restrictions apply.

with annealing times of $16\,\mathrm{h}$ and $30\,\mathrm{h}$. This did not result in larger strains, as seen in Fig. 10.

The elastic strain was predicted well by the model where plasticity in silicon was disabled for most oxidation temperatures. The model underpredicted the elastic strain for oxidation at $900\,^{\circ}\mathrm{C}$, and overpredicted elastic strain for oxidation at $1100\,^{\circ}\mathrm{C}$ with large A_r.

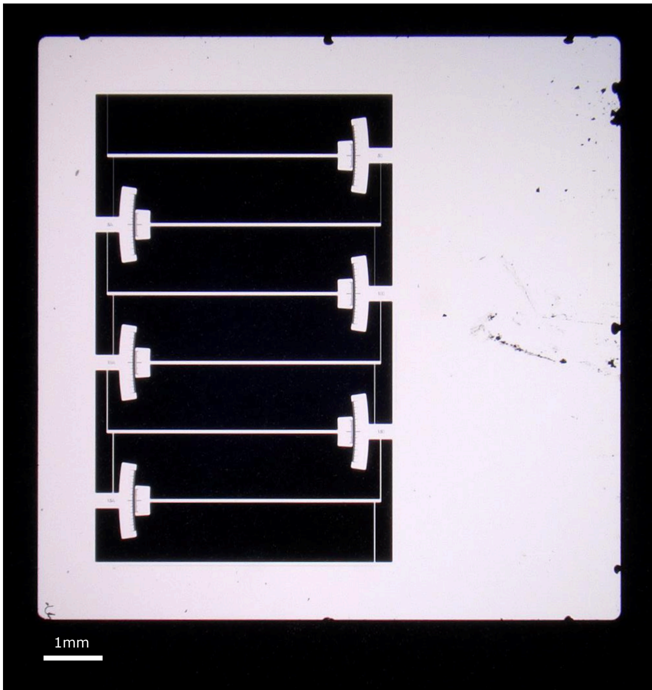

Fig. 4: Optical micrograph of a sample.

IV. Discussion

We have successfully measured both elastic and plastic strain in silicon beams as a result of thermal oxidation.

The maximum observed plastic strain was $0.006\,\%$, which is about 10 times less than predicted. We have performed experiments with multiple oxidation temperatures for different beam widths. The oxidation temperature and beam width influence the measured elastic strain, but do not influence the measured plastic strains. Attempts to induce more plastic strain were made by growing extra thick $2\,\mu\mathrm{m}$ oxide at $1100\,^{\circ}\mathrm{C}$, and by longer annealing. However, the observed plastic strains were still in the same range.

It was assumed that the initial dislocation density was in the order of $1 \times 10^4\,\mathrm{cm}^{-2}$, which is a common value for single crystal silicon in literature [36]–[39]. Lowering the dislocation density in the model would still not explain the observed results, as the model is very insensitive for the initial dislocation density because of the large annealing times. This can be seen in Fig. 3. For an extremely low dislocation density of $0.1\,\mathrm{cm}^{-2}$, the model predicts the same order of plastic strain as for a dislocation density of $1 \times 10^4\,\mathrm{cm}^{-2}$. For reference, in a $10\,\mu\mathrm{m}$ width beam, $0.1\,\mathrm{cm}^{-2}$ means a total of $0.5\,\mathrm{nm}$ dislocation length. This is equal to the silicon crystal lattice spacing, so this could be seen as the minimum possible nonzero dislocation length.

With the AH plasticity model used in this work, a zero dislocation density would predict zero plastic strain. Even though, zero dislocations have been measured in epitaxially grown silicon with special heat treatment [40]. It is unlikely that there are zero crystal defects or impurities at all that can function as dislocation sources in any of our samples. It would also fail to explain the small trend of plastic strain that is observed in the measurements.

The AH model is validated for dislocation densities in the order of $1 \times 10^4\,\mathrm{cm}^{-2}$ to $1 \times 10^6\,\mathrm{cm}^{-2}$ [41]. The model may not be valid for extremely low or zero dislocation densities. For instance, the assumptions of uniformly distributed dislocations may be violated or the assumed multiplication mechanisms may be invalid at extremely low dislocation densities. The agreement between experimental elastic deformation and the model results confirm reliable measurements of deformations, confirming that the model for plastic deformation is most likely invalid. Future research on plasticity in epitaxial silicon by means of tensile or compression tests could provide insight in the observed results in this work. Also measuring the dislocation density and experimenting with doping could shed more light.

We have shown that the lever mechanism was able to distinguish elastic and plastic strain as a result of thermal oxidation. However, the observed plastic strains were smaller than the lever mechanism was designed for. Future research should evaluate the performance for larger plastic strains. This could be achieved by using silicon with more initial dislocations. As previous research by the authors has shown, FZ grown silicon could be used to achieve this. Another option is to use a high level of boron doping in the epitaxial silicon layer. Plastic deformation has been observed in heavily boron doped oxidized silicon membranes [4].

Elastic strain between $0.019\,\%$ and $0.135\,\%$ are measured. Elastic strain measurements are generally in good agreement with the model, where the plasticity of silicon was disabled by simulating with an initial dislocation density of zero. Because plastic strain works stress relieving, the model including plasticity predicts lower elastic strain. At lower oxidation temperatures, the measured elastic strains are significantly larger than predicted. It is likely that at these oxidation temperatures, the stress from volume increase of the oxide is not completely relieved by the viscosity of the oxide. This is in agreement with literature [24], which states that the oxide grows stress-free above $950\,^{\circ}\mathrm{C}$ to $975\,^{\circ}\mathrm{C}$. The assumption of stress free oxide growth is thus invalid for the oxidations at $900\,^{\circ}\mathrm{C}$ and $950\,^{\circ}\mathrm{C}$ and questionable for $1000\,^{\circ}\mathrm{C}$. For more accurate predictions at lower oxidation temperatures, this should be included in the model.

V. Conclusion

A lever mechanism was used to successfully measure both elastic and plastic strain in silicon beams as a result of thermal oxidation. Measurements for different beam width ($5\,\mu\mathrm{m}$ to $15\,\mu\mathrm{m}$) and oxidation temperatures ($900\,^{\circ}\mathrm{C}$ to

Authorized licensed use limited to: TU Delft Library. Downloaded on February 18,2021 at 07:29:10 UTC from IEEE Xplore. Restrictions apply.

TABLE I: Process data

Oxidation temperature	Annealing time	Target thickness	Oxide thickness	<100> beam width in µm			<110> beam width in µm		
900 °C	60 h	1 µm	801 nm	5.35	10.30	15.25	5.84	10.15	15.51
950 °C	16 h	1 µm	940 nm	5.30	10.19	15.18	5.50	10.41	15.50
1000 °C	16 h	1 µm	965 nm	5.47	10.49	15.39	4.97	10.13	14.95
1050 °C	16 h	1 µm	986 nm	5.06	10.08	15.03	5.18	10.18	15.06
1100 °C	16 h	1 µm	1004 nm	4.42	9.70	14.67	4.90	9.71	14.91
1100 °C	16 h	2 µm	1994 nm	2.92	7.73	12.67	2.80	7.51	12.49
1100 °C	30 h	2 µm	1996 nm	2.91	7.85	12.56	2.81	7.72	12.74

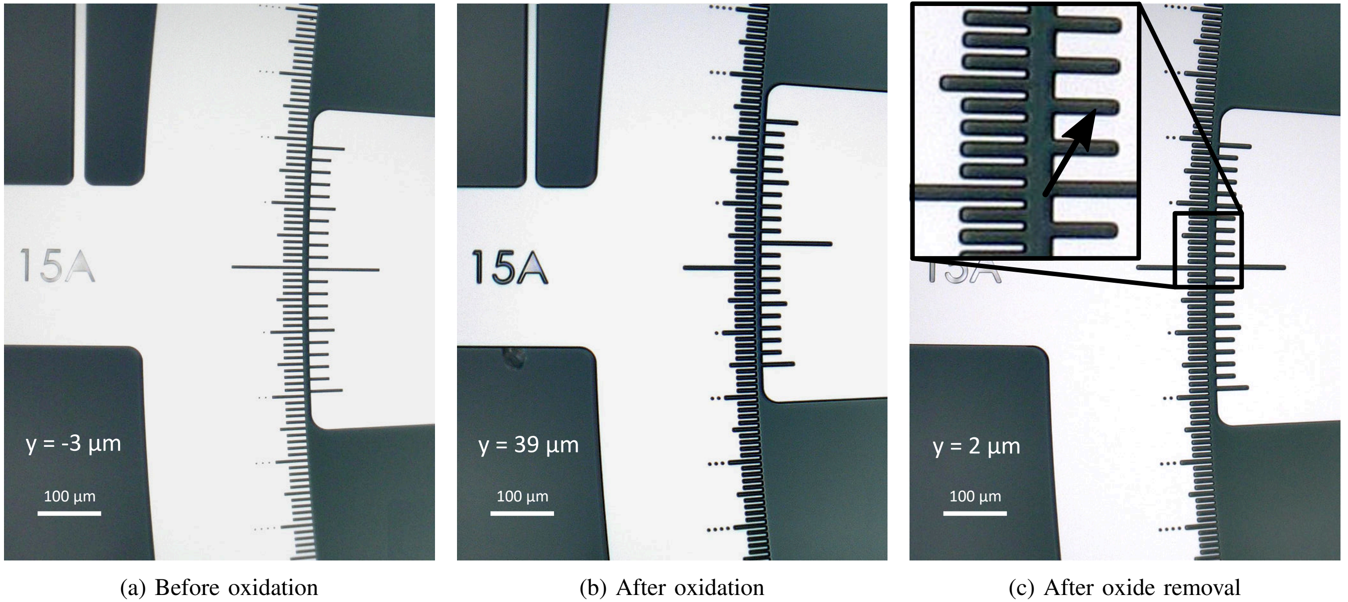

(a) Before oxidation (b) After oxidation (c) After oxide removal

Fig. 5: Example of a measurement read out. A measurement from a 15 µm beam aligned to the <110> direction, 2 µm thick oxide grown at 1100 °C. Fig. 5a shows the initial read out, Fig. 5b shows the read out of the total strain, and Fig. 5c read out after oxide removal. The plastic deformation at the tip is thus 5 µm (0.006 % strain), and the elastic deformation 37 µm(0.048 % strain).

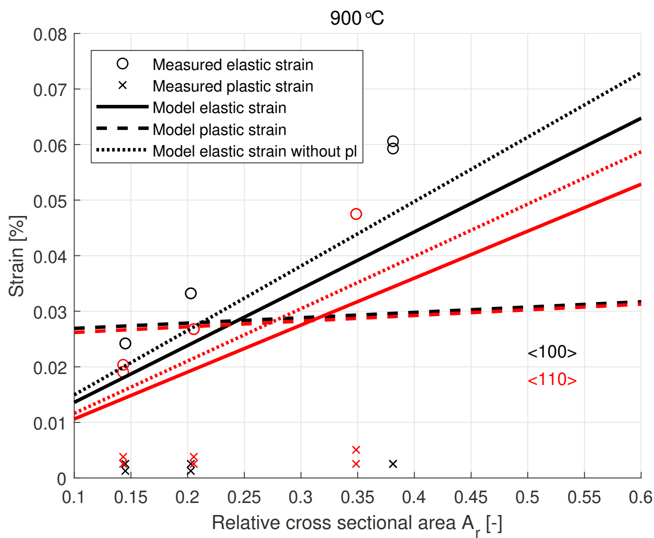

Fig. 6: Experimental and model results for elastic and plastic strain for oxidation at 900 °C.

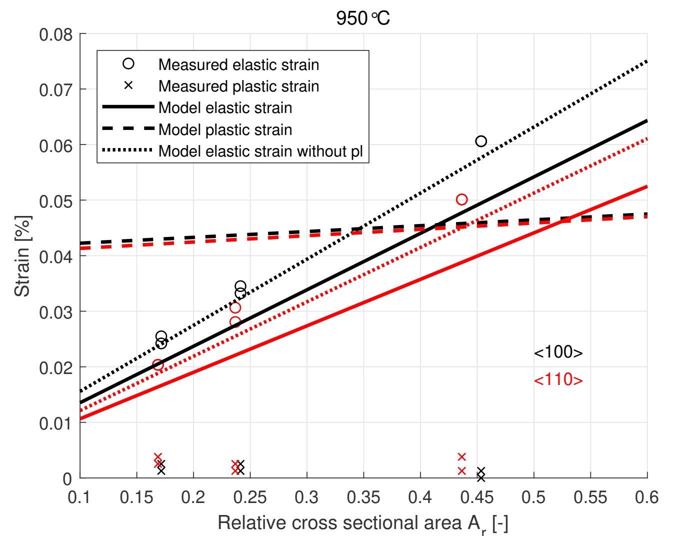

Fig. 7: Experimental and model results for elastic and plastic strain for oxidation at 950 °C.

Authorized licensed use limited to: TU Delft Library. Downloaded on February 18,2021 at 07:29:10 UTC from IEEE Xplore. Restrictions apply.

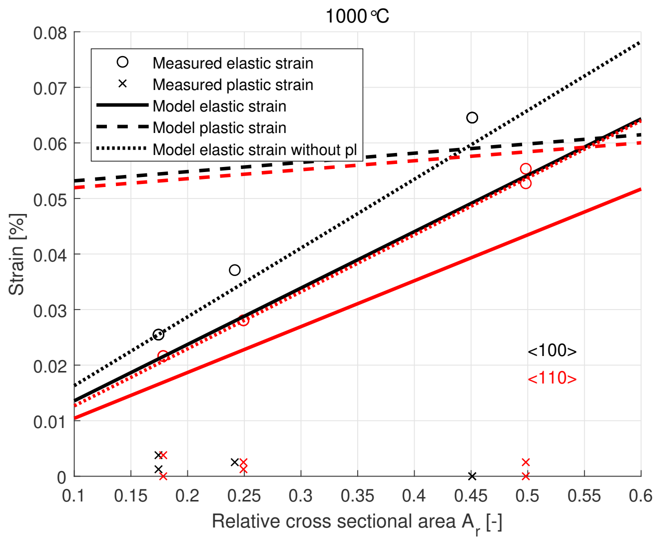

Fig. 8: Experimental and model results for elastic and plastic strain for oxidation at 1000 °C.

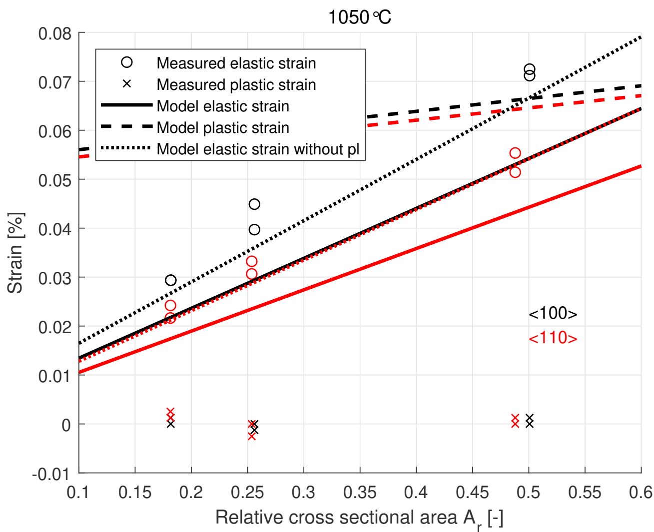

Fig. 9: Experimental and model results for elastic and plastic strain for oxidation at 1050 °C.

1100 °C) have shown significant influence on elastic strain but not on plastic strain.

The maximum plastic strain was 0.006 %, which is significantly less than predicted by the model. Our work suggests that the AH model is not accurate for epitaxial silicon which literature shows has low or zero initial dislocations.

Elastic strain from 0.019 % to 0.135 % was measured, which agrees well with the model for oxidation temperatures from 950 °C to 1100 °C. For oxidation at 900 °C, the model underestimates elastic strain because intrinsic stress originating from for example volume expansion of silicon dioxide during growth is neglected.

We conclude that epitaxial silicon is a good choice when plastic deformation is to be avoided in stress engineering applications. More research is needed in epitaxial silicon for

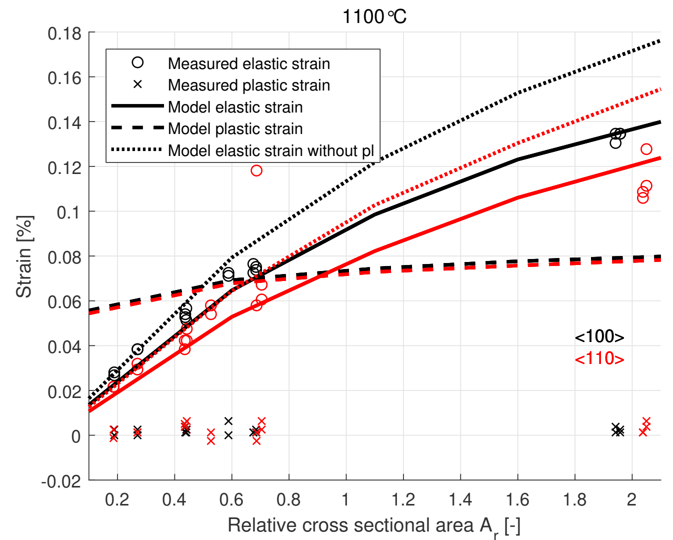

Fig. 10: Experimental and model results for elastic and plastic strain for oxidation at 1100 °C.

more accurate constitutive plasticity models.

Acknowledgments

The authors would like to thank Else Kooi Laboratory, in particular Jia Wei, for help with fabrication and experiments.

References

[1] Y. Zhang and Y. Zhao, "An effective method of determining the residual stress gradients in a micro-cantilever," *Microsyst Technol*, vol. 12, 2006.

[2] C.-Y. Liu, F. Yang, C.-C. Teng, and L.-S. Fan, "A contact-lens-shaped ic chip technology," *J Micromech Microeng*, vol. 24, 2014.

[3] S. Lee, T. Tanaka, and K. Inoue, "Residual stress influences on the sensitivity of ultrasonic sensor having composite membrane structure," *Sens Actuators A Phys*, vol. 125, 2006.

[4] F. Maseeh and S. D. Senturia, "Plastic deformation of highly doped silicon," Massachusetts Inst of Tech, Tech. Rep., 1989.

[5] J. Rabier, P. Renault, D. Eyidi, J. Demenet, J. Chen, H. Couvy, and L. Wang, "Plastic deformation of silicon between 20 c and 425 c," *physica status solidi (c)*, vol. 4, 2007.

[6] Y. J. Tang, J. Chen, Y. B. Huang, S. S. Wang, Z. H. Li, W. D. Zhang *et al.*, "Ultra-sensitive, highly reproducible film stress characterization using flexible suspended thin silicon plates and local curvature measurements," *J Micromech Microeng*, vol. 17, 2007.

[7] M. Finot, I. Blech, S. Suresh, and H. Fujimoto, "Large deformation and geometric instability of substrates with thin-film deposits," *Journal of Applied Physics*, vol. 81, 1997.

[8] G. G. Stoney, "The tension of metallic films deposited by electrolysis," *Proc R Soc Lond A*, vol. 82, 1909.

[9] J. Laconte, F. Iker, S. Jorez, N. André, J. Proost, T. Pardoen, D. Flandre, and J.-P. Raskin, "Thin films stress extraction using micromachined structures and wafer curvature measurements," *Microelectronic engineering*, vol. 76, 2004.

[10] H. Guckel, D. Burns, C. Rutigliano, E. Lovell, and B. Choi, "Diagnostic microstructures for the measurement of intrinsic strain in thin films," *J Micromech Microeng*, vol. 2, 1992.

[11] H. Guckel, T. Randazzo, and D. Burns, "A simple technique for the determination of mechanical strain in thin films with applications to polysilicon," *J of App Phy*, vol. 57, 1985.

[12] A. Kumar, X. Zhang, Q. X. Zhang, M. C. Jong, G. Huang, L. W. S. Vincent, V. Kripesh, C. Lee, J. H. Lau, D. L. Kwong *et al.*, "Residual stress analysis in thin device wafer using piezoresistive stress sensor," *IEEE Trans Compon Packaging Manuf Technol*, vol. 1, 2011.

[13] T. C. Lo and P. C. Chan, "Design and calibration of a 3-d micro-strain gauge for in situ on chip stress measurements," in *ICSE*. IEEE, 1996.

Authorized licensed use limited to: TU Delft Library. Downloaded on February 18,2021 at 07:29:10 UTC from IEEE Xplore. Restrictions apply.

[14] N. D. Masters, M. P. de Boer, B. D. Jensen, M. S. Baker, and D. Koester, "Side-by-side comparison of passive mems strain test structures under residual compression," in *Mechanical Properties of Structural Films*. ASTM International, 2001.

[15] A. Horsfall, J. dos Santos, S. Soare, N. Wright, A. O'neill, S. Bull, A. Walton, A. Gundlach, and J. Stevenson, "Direct measurement of residual stress in sub-micron interconnects," *Semicond Sci Technol*, vol. 18, 2003.

[16] F. Ericson, S. Greek, J. Söderkvist, and J.-A. Schweitz, "High-sensitivity surface micromachined structures for internal stress and stress gradient evaluation," *J Micromech Microeng*, vol. 7, 1997.

[17] B. Van Drieënhuizen, J. Goosen, P. French, and R. Wolffenbuttel, "Comparison of techniques for measuring both compressive and tensile stress in thin films," *Sens Actuators A Phys*, vol. 37, 1993.

[18] B. Kämpfe, "Investigation of residual stresses in microsystems using x-ray diffraction," *J Mater Sci Eng A*, vol. 288, 2000.

[19] P. Goudeau, N. Tamura, B. Lavelle, S. Rigo, T. Masri, A. Bosseboeuf, T. Sarnet, J.-A. Petit, and J.-M. Desmarres, "X-ray diffraction characterization of suspended structures for mems applications," 2005.

[20] J. Frühauf, E. Gärtner, and E. Jänsch, "Silicon as a plastic material," *J Micromech Microeng*, vol. 9, 1999.

[21] J. Kim, H. Choo, L. Lin, and R. S. Muller, "Microfabricated torsional actuators using self-aligned plastic deformation of silicon," *J Microelectromech Syst*, vol. 15, 2006.

[22] M. W. Judy, Y.-H. Cho, R. T. Howe, and A. P. Pisano, "Self-adjusting microstructures (sams)," in *Proc IEEE Micro Electro Mech Syst*. IEEE, 1991.

[23] B. A. Boom, A. Bertolini, E. Hennes, R. A. Brookhuis, R. J. Wiegerink, J. Van den Brand, M. Beker, A. Oner, and D. Van Wees, "Nano-g accelerometer using geometric anti-springs," in *Proc IEEE Int Conf Micro Electro Mech Syst*. IEEE, 2017.

[24] E. EerNisse, "Stress in thermal sio2 during growth," *Applied Physics Letters*, vol. 35, 1979.

[25] A. Masolin, P.-O. Bouchard, R. Martini, and M. Bernacki, "Thermo-mechanical and fracture properties in single-crystal silicon," *Journal of Materials Science*, vol. 48, 2013.

[26] B. E. Deal and A. Grove, "General relationship for the thermal oxidation of silicon," *Journal of Applied Physics*, vol. 36, 1965.

[27] B. Gao, S. Nakano, H. Harada, Y. Miyamura, and K. Kakimoto, "Effect of cooling rate on the activation of slip systems in seed cast-grown monocrystalline silicon in the [001] and [111] directions," *Crystal Growth & Design*, vol. 13, 2013.

[28] E. Orowan, "Problems of plastic gliding," *Proceedings of the Physical Society*, vol. 52, 1940.

[29] I. Yonenaga and K. Sumino, "Dislocation dynamics in the plastic deformation of silicon crystals ii. experiments," *Physica status solidi (a)*, vol. 51, 1979.

[30] E. Irene, E. Tierney, and J. Angilello, "A viscous flow model to explain the appearance of high density thermal sio2 at low oxidation temperatures," *J Electrochem Soc*, vol. 129, 1982.

[31] M. A. Hopcroft, W. D. Nix, and T. W. Kenny, "What is the young's modulus of silicon?" *J Microelectromech Syst*, vol. 19, 2010.

[32] C. Bourgeois, E. Steinsland, N. Blanc, and N. De Rooij, "Design of resonators for the determination of the temperature coefficients of elastic constants of monocrystalline silicon," in *Frequency Control Symposium*. IEEE, 1997.

[33] A. K. Swarnakar, O. Van der Biest, and J. Vanhellemont, "Determination of the si young's modulus between room and melt temperature using the impulse excitation technique," *physica status solidi (c)*, vol. 11, 2014.

[34] H. Tada, A. E. Kumpel, R. E. Lathrop, J. B. Slanina, P. Nieva, P. Zavracky, I. N. Miaoulis, and P. Y. Wong, "Thermal expansion coefficient of polycrystalline silicon and silicon dioxide thin films at high temperatures," *J Appl Phys*, vol. 87, 2000.

[35] Y. Okada and Y. Tokumaru, "Precise determination of lattice parameter and thermal expansion coefficient of silicon between 300 and 1500 k," *Journal of Applied Physics*, vol. 56, 1984.

[36] K. Sumino and I. Yonenaga, "Difference in the mechanical strengths of dislocation-free crystals of czochralski silicon and float-zone silicon," *Jpn J Appl Phys*, vol. 20, 1981.

[37] J. Cochard, I. Yonenaga, S. Gouttebroze, M. MHamdi, and Z. Zhang, "Constitutive modelling of silicon: Parameters identification of classical models using crystal plasticity," 2009.

[38] J. Ren, M. Ward, P. Kinnell, and R. Cradock, "Finite element modeling for the mechanical behavior of silicon diaphragms using comsol multiphysics."

[39] H.-S. Moon, L. Anand, and S. Spearing, "A constitutive model for the mechanical behavior of single crystal silicon at elevated temperature," *Mater Res Soc Symp Proc*, vol. 687, 2001.

[40] H. Sugiura and M. Yamaguchi, "Growth of dislocation-free silicon films by molecular beam epitaxy (mbe)," *Journal of Vacuum Science and Technology*, vol. 19, 1981.

[41] I. Yonenaga and K. Sumino, "Dislocation dynamics in the plastic deformation of silicon crystals i. experiments," *Physica status solidi (a)*, vol. 50, 1978.

Authorized licensed use limited to: TU Delft Library. Downloaded on February 18,2021 at 07:29:10 UTC from IEEE Xplore. Restrictions apply.